OPEN

Light: Science & Applications (2015) 4, e267; doi:10.1038/lsa.2015.40

www.nature.com/lsa

ORIGINAL ARTICLE

Bioinspired optical antennas: gold plant viruses

SoonGweon Hong[1,2], Mi Yeon Lee[3], Andrew O Jackson[3] and Luke P Lee[1,2,4,5]

The ability to capture the chemical signatures of biomolecules (i.e., electron-transfer dynamics) in living cells will provide an entirely new perspective on biology and medicine. This can be accomplished using nanoscale optical antennas that can collect, resonate and focus light from outside the cell and emit molecular spectra. Here, we describe biologically inspired nanoscale optical antennas that utilize the unique topologies of plant viruses (and thus, are called gold plant viruses) for molecular fingerprint detection. Our electromagnetic calculations for these gold viruses indicate that capsid morphologies permit high amplification of optical scattering energy compared to a smooth nanosphere. From experimental measurements of various gold viruses based on four different plant viruses, we observe highly enhanced optical cross-sections and the modulation of the resonance wavelength depending on the viral morphology. Additionally, in label-free molecular imaging, we successfully obtain higher sensitivity (by a factor of up to 10^6) than can be achieved using similar-sized nanospheres. By virtue of the inherent functionalities of capsids and the plasmonic characteristics of the gold layer, a gold virus-based antenna will enable cellular targeting, imaging and drug delivery.
Light: Science & Applications (2015) **4,** e267; doi:10.1038/lsa.2015.40; published online 27 March 2015

Keywords: molecular sensor; nanophotonics; optical antenna; optical spectroscopy; plant virus; plasmonics; plasmonic resonant energy transfer (PRET); surface enhanced Raman scattering (SERS)

INTRODUCTION

In current nanotechnology, the development of nanoscale optical antennas that are capable of receiving and transmitting light in unique light–electron interactions called 'surface plasmons'[1] is of considerable interest because of the potential applications of such antennas in molecular detection,[2–4] multiple harmonic generation,[5,6] plasmonic photovoltaics,[7] optoelectronics,[8] negative-index materials[9] and more. In particular, the use of an optical antenna as a molecular sensor permits the dynamic detection of chemical signatures in a non-invasive and label-free manner. Moreover, the detection sensitivity can reach the single-molecule level.[3,10] These powerful characteristics distinguish the optical antenna as a potential method for unraveling the inherent complexity of biological systems (i.e., cells), which is a difficult task using current techniques.

To be suitable for use as a biomolecular sensor in cellular systems, an optical antenna should not interfere with cellular components and should be efficiently accessible (or mobile) to subcellular regions. These characteristics can be achieved by exploiting the nanoscale size and chemical stability of non-fixed, biochemical-moiety-containing nanoparticles. In this context, gold nanospheres have been successfully demonstrated to be capable of actively targeting subcellular regions and carrying imaging agents and drugs.[11,12] However, the smooth surfaces of chemically synthesized gold nanoparticles do not impart these nanoparticles with ideal functionality for molecular fingerprint detection. Optically amplified hot spots, which can generate molecular fingerprint spectra in far-field scattering signals, are strongly induced near sharp tips or at close tip-to-tip distances in nanoscale features, which chemically synthesized nanoparticles lack. However, viruses, which are common natural nanoparticles, present an ideal morphology for molecule-sensing antennas.

Viruses are highly ordered natural nanoarchitectures that consist of nucleic acid and a protective coat protein called a capsid. Even with their simple composition, viruses have evolved to attain the capability to enter a cell and utilize the host to replicate their genomes, re-assemble, and disseminate their progeny. Over the past century, these processes have been extensively studied to achieve better control of viral diseases, especially in plants; moreover, at present, attempts are being made in nanotechnology and biotechnology to engineer viruses for diagnostic/therapeutic applications,[13–17] nanomaterial synthesis,[18,19] protein recombination,[20,21] energy harvesting,[22,23] and even the fabrication of electronic components.[24,25] These new approaches to virus engineering involve eliminating the viral disease-causing characteristics or, more accurately, incorporating only the inherent circulatory and targeting capabilities of viruses into the design of applications.

The capsids of viruses, rather than their nucleic acids, have received particular attention in virus engineering because of their various appealing features, including self-assembly, regular geometries, a high degree of symmetry and polyvalency, and stability in harsh extracellular environments.[26–29] Moreover, the morphological unit of a capsid, called a capsomer, can be chemically or genetically manipulated to carry external materials (i.e., diagnostic/imaging agents, therapeutic payloads, inorganic materials). Capsomers with distinguishable carrying spots

[1]Department of Bioengineering, University of California at Berkeley, Berkeley, CA 94720, USA; [2]Berkeley Sensor and Actuator Center, University of California at Berkeley, Berkeley, CA 94720, USA; [3]Department of Plant & Microbial Biology, University of California at Berkeley, Berkeley, CA 94720, USA; [4]Department of Electrical Engineering and Computer Sciences, University of California at Berkeley, Berkeley, CA 94720, USA and [5]Biophysics Graduate Program, University of California at Berkeley, Berkeley, CA 94720, USA
Correspondence: LP Lee, Department of Electrical Engineering and Computer Sciences, University of California at Berkeley, Berkeley, CA 94720, USA.
E-mail: lplee@berkeley.edu
Received 5 September 2014; revised 30 December 2014; accepted 11 January 2015; accepted article preview online 13 January 2015

and multiple protein domains offer increased potential for the use of viruses as ideal multifunctional nanoparticles. The somewhat simple configuration of capsids has been extended in utility from simply protecting the viral genome to addressing obstacles hindering the realization of ideal nanomaterials.

The research presented here also concerns viral capsids but focuses on their detailed structures. A close examination of viral capsid structures reveals very attractive subnanometer or molecular-level architectures.[29] Previously, surface-roughened nanoparticles have been demonstrated to act as sensitive optical antennas in molecular detection, with potential for use in the imaging of living cells.[30,31] However, the achievement of subnanometer resolution and three-dimensional details, along with good regularity and uniformity, on the nanometer-sized scale of viral particles is certainly beyond the capabilities of current nanofabrication techniques. We propose that the unique and detailed structures of viral capsids can be used as strong plasmonic templates by conjugating novel metals onto their surfaces. The plasmonic metal layer formed in this manner will function as an optical antenna to amplify and convert incident light into confined nanoscale volumes.[32] The combination of optical antennas and viruses offers a critical solution for sending optical antennas (or nanosatellites) into living cells (or cellular galaxies) and retrieving valuable information (as from satellites orbiting a planet).

MATERIALS AND METHODS

Virus sample preparation

Plant leaves with the symptoms of viral infection were harvested 1 or 2 weeks after mechanical inoculation. Then, the viruses were purified from the infected leaves using standard methods described in previous publications.[33] The harvested viruses were stored at −20 ℃ with the addition of 5% ethylene glycol until their usage. Viruses can be stored in this manner for many years while remaining infectious.

Fabrication of gold viruses

A conventional electron-beam evaporator as used to deposit various thicknesses (2–10 nm) of gold onto viruses electrostatically conjugated on a clean glass slide. For the control experiments, polystyrene beads of 33 nm in diameter (Duke Scientific Corp., Palo Alto, CA, USA) were prepared in the same manner and deposited using the same procedure. To decrease the temperature during the deposition (<55 ℃) and increase the directionality of deposition, the evaporation was performed under high vacuum ($<4\times10^{-6}$ torr), and the deposition rate was high ($\sim$0.5 nm s^{-1}). After deposition, lift-off was performed in water *via* pH adjustment and weak sonication, followed by reattachment on thiol-functionalized glass using 3-mercaptopropyl-trimethoxy-silane for the optical characterization of the monodisperse nanoparticles (Supplementary Fig. S4).

Electromagnetic simulations of the gold viruses

A morphological description of an intriguing capsid model (Equation (1)) was referenced from a previous publication.[34] For the gold virus model, one set of variables (*m*, *p*, *const*) in Equation (1) was chosen to express the three-dimensional protrusions and valleys of the capsids, and a gold layer of 5 nm in thickness was assumed to be normally deposited with appropriate directionality.

$$\sum_{n=-m}^{m} e^{-(x+\tau y-n)^p}+e^{-(x-\tau y-n)^p}+e^{-(y+\tau z-n)^p}+e^{-(y-\tau z-n)^p} +e^{-(z+\tau x-n)^p}e^{-(z-\tau x-n)^p}-const=0 \quad (1)$$

A representative cross-section of the capsid model was input into the two-dimensional module of a COMSOL RF (radiofrequency) simulation (ver. 3.5a). The permittivity of the gold layer was obtained from a modified Drude model,[35] and that of the virus and nanosphere templates was assumed to be equivalent to that of polystyrene (ε_r=2.5). For analytical comparison of the optical characteristics, the radiative energy and resistive energy were calculated based on Equation (2).[36]

$$P_{\text{Total}} = P_{\text{radiative}} + P_{\text{resistive}} = \int_V \mathbf{H}\cdot\frac{\partial \mathbf{B}}{\partial t}\,\mathrm{d}V + \int_V \mathbf{E}\cdot\frac{\partial \mathbf{D}}{\partial t}\,\mathrm{d}V = \oint_S (\mathbf{E}\times\mathbf{H})\cdot\mathbf{n}\,\mathrm{d}S + \int_V \mathbf{J}\cdot\mathbf{E}\,\mathrm{d}V \quad (2)$$

where **H** is the magnetic field, **B** is the magnetic flux, **E** is the electric field, **D** is the electric displacement and **J** is the current density.

Transmission electron microscopy (TEM)

An FEI Tecnai 12 TEM operated at 100 kV was used for negative-staining imaging of both the innate and engineered viruses. The gold-coated virus samples were released from the support surface and transferred to a carbon-coated copper grid. The samples were washed with distilled water and negatively stained with an aqueous solution of 1% uranyl acetate for 1 min.[37]

Dark-field scattering spectrum

An inverted microscope (Carl Zeiss Axiovert 200) equipped with a dark-field condenser lens (1.2<NA<1.4) and a spectrometer (Princeton Instruments Acton SP2300) was used to measure the scattering spectra from individual gold-virus particles. The combination of a slit aperture placed in front of the spectrometer and the use of software to define a 'region of interest' (Winspec; Roper Scientific, Trenton, NJ, USA) was used to confine the imaging area to capture single-particle scattering.[4] Among the variety of spectra recorded because of the close placement of multiple particles and/or the various attachment orientations of the gold-virus particles, the most dominant spectrum (>70%) was chosen to represent the scattering spectrum of each type of gold virus.

Absorption spectrum measurements using gold viruses

Gold-virus particles immobilized on a thiolated substrate were functionalized with 3-mercaptopropylcarboxylic acid *via* incubation in 1 mM mercaptopropylcarboxylic acid isopropyl alcohol for 24 h. A reduced form of cytochrome c (or cyt c; Sigma, St Louis, MO, USA), which was sold in the oxidized form, was obtained through the addition of excess sodium dithionite ($Na_2S_2O_4$) in deoxygenated PBS buffer solution, as described previously.[4] Dark-field scatterings were measured on the functionalized gold-virus particles incubated in cyt c solutions. The measured scattering spectra were post-processed to analyze the quenching intensities through the observation of the plasmon resonance energy transfer between the cyt c and gold-virus particles.

Vibration spectrum measurement using gold viruses

A Raman molecule, 1,2-bis(4-pyridyl)ethylene (BPE), was further purified using a conventional re-crystallization process.[38] Then, three independent sets of methanol-based BPE solutions with concentrations from 1 mM to 1 fM were prepared *via* gradual dilutions and tested. A monodisperse form, as shown in Supplementary Figs. S4c and S5b, was used as the surface enhanced Raman scattering substrate. Optical scattering characterization indicated that the cowpea mosaic virus with a gold layer of 2 nm in thickness was matched to an optical resonance at a wavelength of 785 nm. A Raman microscope was

doi:10.1038/lsa.2015.40

assembled from an inverted Carl Zeiss microscope with a 785 nm diode laser (Power Technology, Inc., Alexander, AR, USA) and a 785 nm Raman filter set. Using a neutral density filter, the intensity of the laser was adjusted to prevent damage to the particles and to avoid bubble generation caused by overheating.

RESULTS AND DISCUSSION

Herein, we characterize the potential for the use of virus morphology in molecular spectroscopic detection. Previous investigations using electron microscopy have demonstrated that virus particles have highly ordered natural nanoarchitectures, with a coat protein called a capsid.[39] The external surface of a viral capsid commonly contains protrusions and valleys on the subnanometer scale, precisely the morphology required for optical antennas. Moreover, viral reproduction yields a remarkably high degree of symmetry and uniformity that is beyond the capability of current nanotechnology. These characteristics make viral nanoparticles attractive templates for optical antennas. Additionally, infection selectivity and recent engineering endeavors to eliminate harmful viral effects have enabled the utility of various viral particles in human-involved applications, such as therapeutics. Thus, we can take advantage of the morphological characteristics of plant viruses by integrating novel metals onto the external surfaces of their capsids for highly sensitive and selective molecular spectroscopic detection (i.e., localized electronic absorption and vibration spectroscopy) (Figure 1).

In addition to using virus morphology for detection sensitivity, resonance wavelength selectivity for various optical sensing applications can also be achieved in this manner. Similar to a macroscale RF antenna, an optical antenna requires the modulation of its resonance wavelength based on application conditions (i.e., the optical properties of the target molecule and the wavelength of optical excitation).[4,40] Nature provides millions of different capsid topologies, and the advancements in biological electron microscopy and X-ray crystallography achieved in recent decades have allowed for the classification of these diverse morphologies. Thus, overlaying a novel metal layer onto well-characterized virus particles can achieve the two prerequisites for a molecule-detecting antenna, namely, detection sensitivity and wavelength selectivity (Figure 1d). Engineered viral particles, especially when utilized in different types of hosts than those for which the corresponding viruses evolved (i.e., plant viruses introduced into mammalian cells), can eliminate biological hazards and enable the utilization of either inherent or endowed biochemical properties of the viral capsids to target subcellular regions.[41] Thus, our gold viruses can exploit the molecular-sensing capability of optical antennas and the biochemical properties of viral capsids, which have been demonstrated previously for decoupled targeting and sensing.[31]

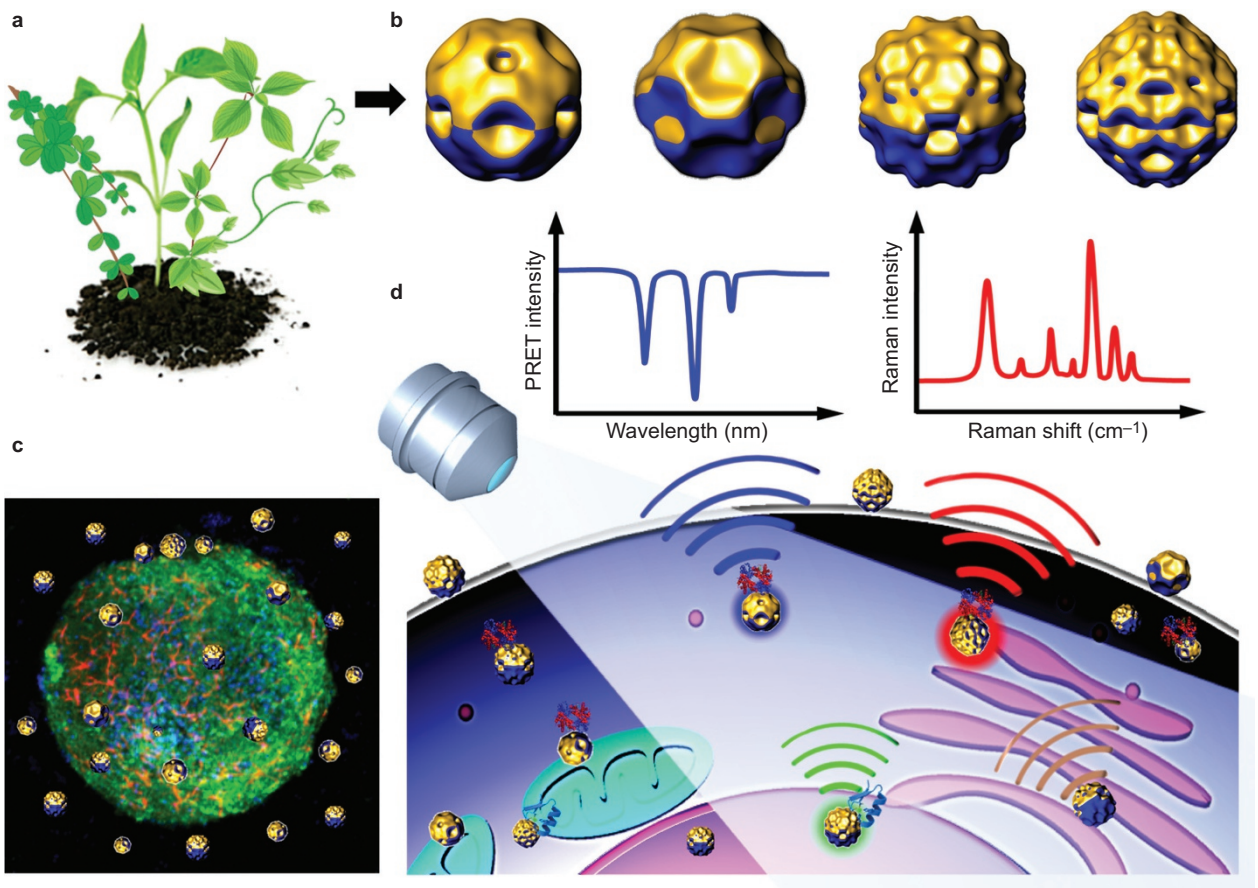

Figure 1 Schematic illustrations of the use of gold viruses for molecular imaging. From various plant hosts (**a**), various gold viruses can be generated through an engineering process of gold conjugation (**b**). The morphological delicacy of viral capsids enables sensitivity in detection, and the variety of viral morphologies that have arisen through natural evolution allows for a broad range of wavelength selectivity among molecule-detecting optical antennas. Thus, it can be envisioned that various gold viruses can potentially function as optical nanosatellites in a biological galaxy such as cellular tissues (**c**) and intracellular spaces (**d**), exhibiting various biomolecular imaging capabilities with detection sensitivity. PRET, plasmonic resonant energy transfer.

The development of mathematical models of virus capsids could also enhance the potential for the application of viruses in molecular spectroscopic imaging. As an important aspect of viral studies, mathematical models have been developed to gain a fundamental understanding of viral structural and morphological analyses, classifications and applications.[26,34,42,43] These models can facilitate electromagnetic-field calculations of the optical response of a virus-template antenna. Using a topological description of an intriguing capsid model,[34] we characterized the optical properties of our gold viruses compared to gold conjugated onto a smooth nanosphere. The simulation analysis explicitly indicated that the protrusions and valleys of capsid topology lead to the generation of more hot spots near the few-nanometer-distant tips of the gold structures than are created by the smooth surface of a nanosphere, which forms a single dome structure with a single edge (Figure 2). The electromagnetic energy comparison between the two types of structures clearly illustrates the advantages of the virus template. A gold virus generates more radiative energy and less resistive thermal energy in the gold layer (Figure 2c and 2d). Thus, gold viruses can be useful in applications that utilize enhanced optical fields, such as sensitive and selective molecular imaging (i.e., vibration and absorption spectroscopy).[4,44] Moreover, the lower resistive thermal energy may also be beneficial to the structural stability of the gold viruses under light excitation.[45]

As a proof of concept, four types of well-characterized icosahedral plant viruses including belladonna mottle virus, brome mosaic virus, tomato bushy stunt virus and cowpea mosaic virus (CPMV) were purified from infected plants, and thin gold layers of various thicknesses (1–10 nm) were conjugated onto the viruses *via* directional electron evaporation. The structures of the resulting nanoparticles were verified using a TEM. The TEM results indicated that the viruses maintained their original spherical structures and revealed the presence of numerous electron-dense gold particles on each of the virions after gold-layer conjugation (Supplementary Fig. S5b and S5e). To assess whether deposition destroyed the biological activity of the virus, an infectivity assay was conducted by inoculating primary leaves of cowpea (*Vigna unguiculata*) cv. Chinese × Iron plants after the engineering processes were completed.[46] Both the wild-type and gold-virus CPMVs produced similar numbers of necrotic local lesions on the leaves; therefore, the process appeared to have had no substantial effect on the viral activity (Supplementary Fig. S3C and S3F).

Then, the optical properties of these four different gold viruses were characterized by measuring their optical dark-field scattering signals. The dark-field images indicated that the scattering intensities of the gold viruses were one order of magnitude higher than those of both the intact viruses and similar-sized gold nanospheres (Supplementary Fig. S7). Additionally, the four types of gold viruses were observed to have

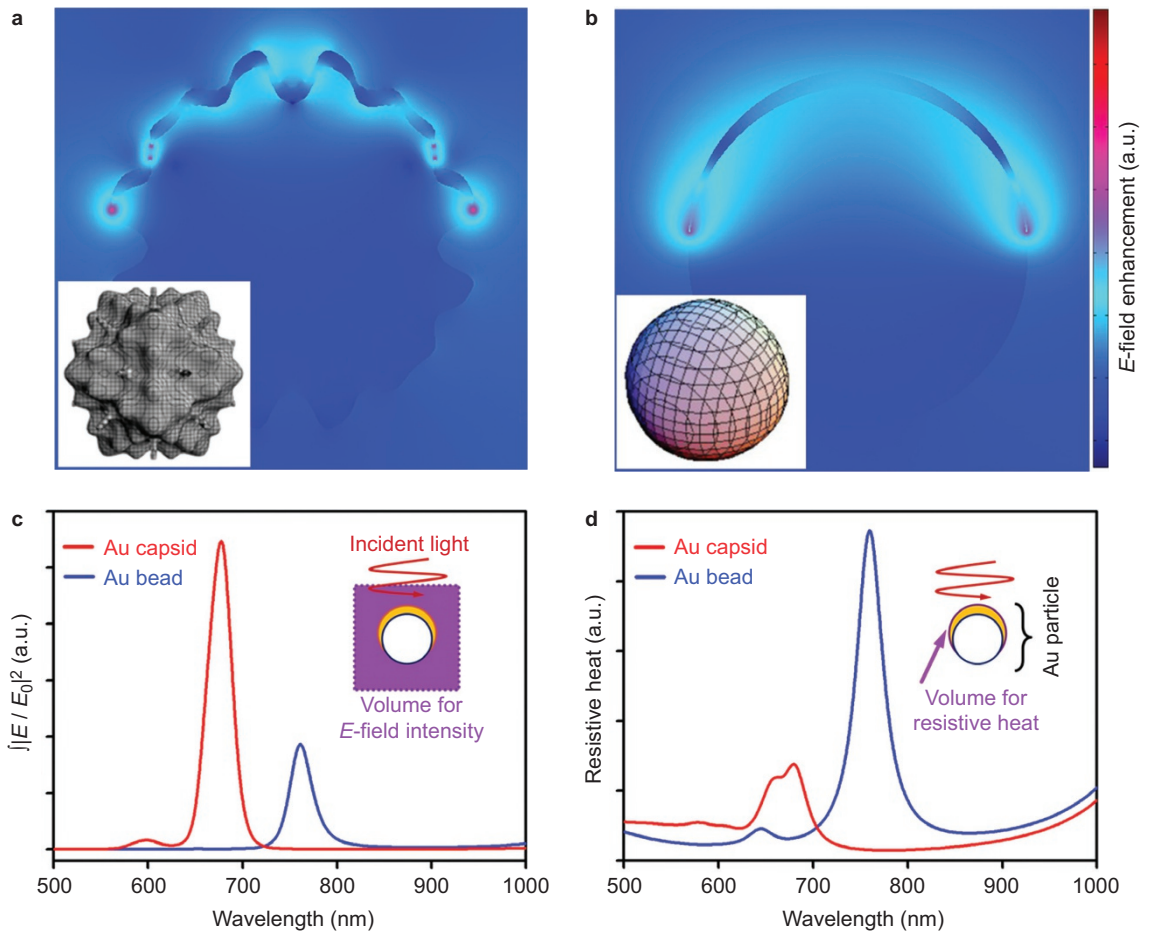

Figure 2 Electromagnetic simulations of a gold virus and a gold-conjugated nanosphere. The representative viral capsid structure was modeled using a mathematical expression presented in a previous publication.[34] Both nanoparticles were scaled to 30 nm in diameter. (**a** and **b**) The capsid morphology generates more optically enhanced spots than does the nanosphere morphology. (**c** and **d**) A comparison of the radiative and resistive energies of the two nanoparticles indicates that the gold virus can enable molecular detection with improved sensitivity and stability.

doi:10.1038/lsa.2015.40

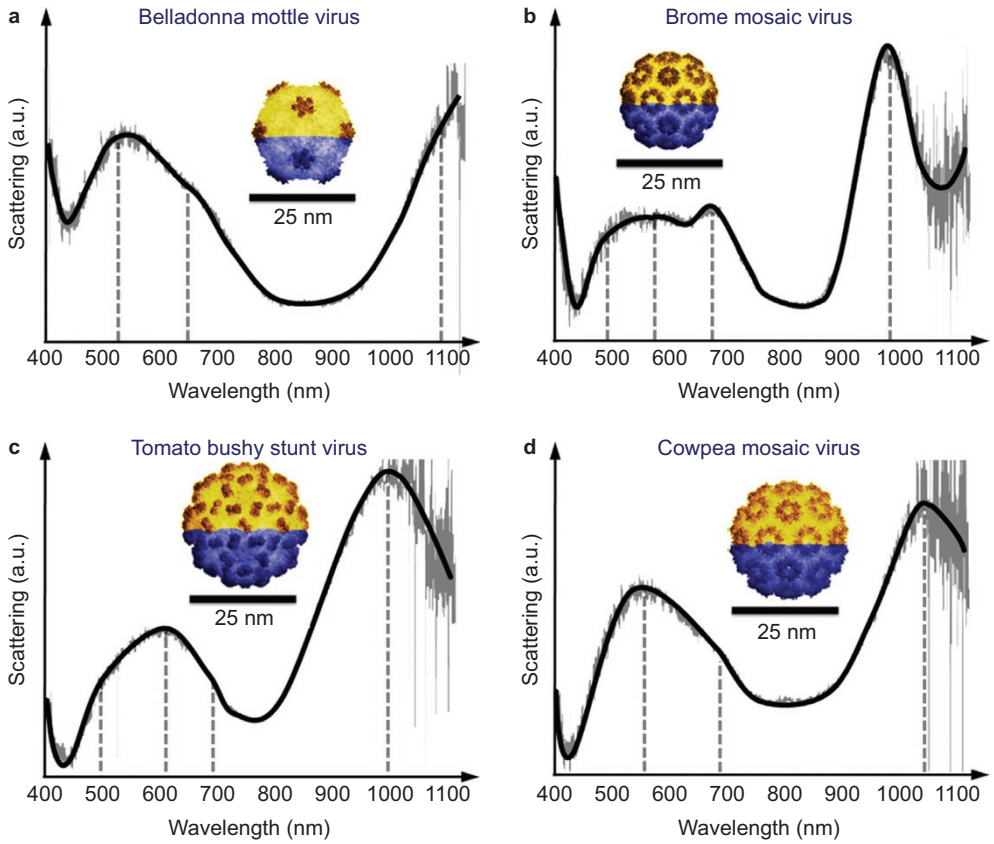

Figure 3 Measurements of the optical properties of various gold plant viruses. (**a**) BdMV, (**b**) BMV, (**c**) TBSV and (**d**) CPMV were conjugated with identical 5-nm gold layers *via* metal evaporation. The particles were prepared as single nanoparticles on a glass substrate for single-particle optical characterization. The optical measurements demonstrate variations in optical resonance frequency that are strongly dependent on the details of the capsid morphology. BdMV, belladonna mottle virus; BMV, brome mosaic virus; CPMV, cow pea mosaic virus; TBSV, tomato bush stunt virus.

distinguishable optical resonances. Although the four types of plant viruses used are similar in size (approximately 30 nm) and identical in symmetry (T=3, where T is the triangulation number[43]), the differences in their morphological details (as shown in the insets of Figure 3) resulted in a modulation of their optical resonances, thereby demonstrating the capability for wavelength selectivity *via* viral template selection. Among the four types of plant viruses, an increased proximity between protruding capsomers results in the clearer manifestation of multiple resonances in the visible range, whereas an increase in diameter generates a red shift in the optical resonance. Moreover, the asymmetric conjugation of the gold layer grants the ability to achieve a wide range of resonance shifts by modifying the thickness of the gold layer (Supplementary Fig. S3). Thus, through the selection of virus type and metal thickness, antennas with a broad range of optical resonances can be fabricated for diverse optical sensing applications.

For molecular imaging using gold virus-based optical antennas, we demonstrated localized electronic absorption spectroscopy *via* a phenomenon called plasmon resonance energy transfer and vibrational spectroscopy *via* surface-enhanced Raman scattering; both methods provide high sensitivity and selective molecular imaging.[3,4] An enhanced electromagnetic field near the excited optical antenna can increase the intensity of vibrational modes and lead to the transfer of excitation energy to nearby molecules, yielding re-scattered signals encoding molecular fingerprints at levels far above that of the background noise. The calculations presented above indicate that the use of a gold virus is beneficial not only in increasing the overall radiative energy but also in creating a highly amplified electromagnetic field at multiple spots, thereby enhancing the spectroscopic results.

When the optical resonances overlap between a metallic nanoparticle and its target molecules, the molecular absorption spectra can be encoded in the scattered signals of the nanoparticle.[4,47,48] Because gold viruses have larger optical cross sections than those of similar-sized nanoparticles, they offer enhanced encoding efficiency. To characterize the sensitivity of gold viruses for the encoding of absorption spectra, one type of gold virus was tested for the detection of cyt c.[4,47] Various concentrations of cyt c were incubated with CPMVs coated with 5 nm of gold, and as a control, gold-coated nanospheres (33-nm-diameter polystyrene beads) were simultaneously examined. Figure 4b and 4c demonstrate that the gold virus allowed for more sensitive detection of the absorption spectrum of cyt c more sensitively than did the smooth nanosphere, yielding approximately 10-fold higher magnitudes. The higher absorption encoding efficiency achieved using the gold virus can be understood as a result of the large number of hot spots that formed on the gold virus, as indicated by the simulation (although the larger surface area of the gold layer on the polymer sphere (33 nm) compared to that of the CPMV virus (31 nm) offered the possibility for the adsorption of more molecules).

The strong electromagnetic fields that form around gold viruses can also permit more sensitive detection in Raman scattering measurements because Raman scattering signals are amplified by $|E|^4$ near metallic nanostructures (where $|E|$ is the magnitude of the electric field).[49] For a general assessment of the efficacy of gold viruses in

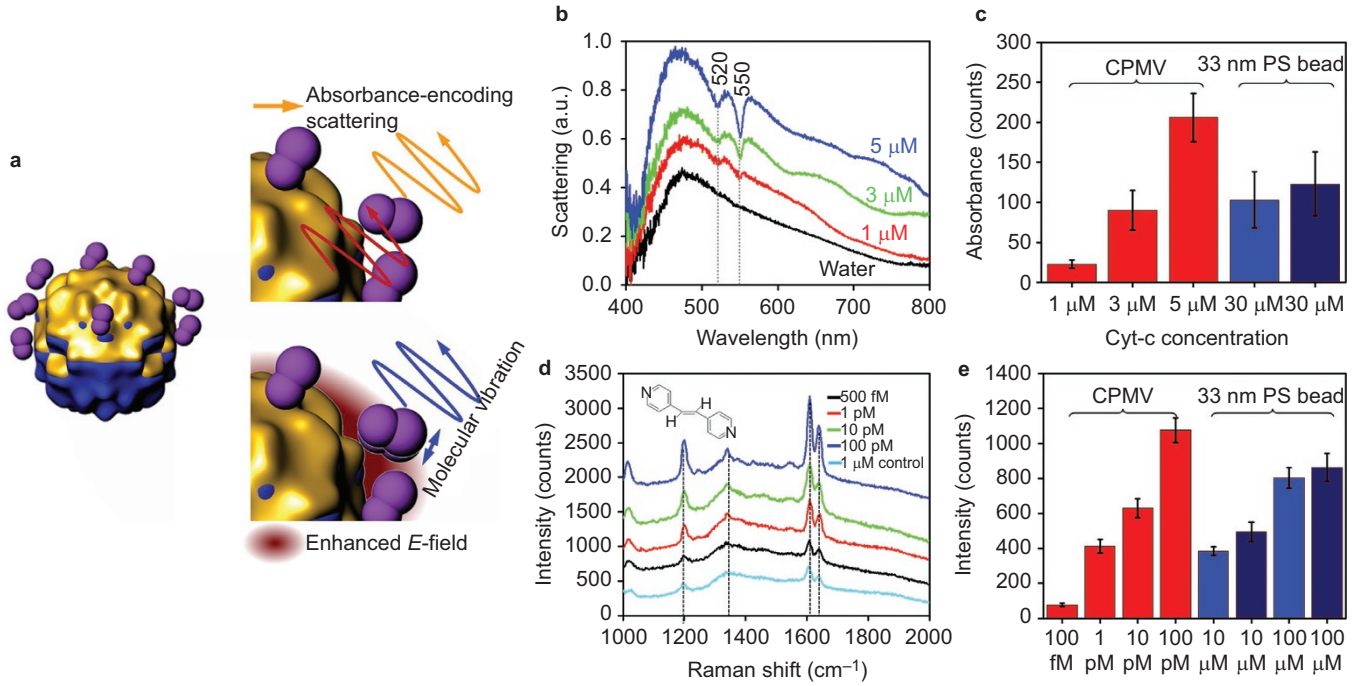

Figure 4 Molecular fingerprint detection using gold viruses. (**a**) The detection of absorption and vibration spectra *via* gold virus scattering. The broad-band light scattering profile is reshaped by efficient optical energy transfer to nearby molecules, thus revealing their absorption spectra. A single-wavelength excitation is sufficiently amplified near the gold virus surface to augment inelastic scattering, thereby revealing the vibrational modes of nearby molecules. (**b**) Cyt c detection *via* CPMVs coated in 5 nm of gold. The absorption spectrum of reduced cyt c was clearly observed from the gold virus scattering spectrum (520- and 550-nm peaks). (**c**) Comparison of the encoding efficiencies of the absorption spectra of a gold virus and two different gold nanospheres. The results for a nanosphere with the same thickness of gold (i.e., 5 nm) and a nanosphere with a gold thickness that reproduces the 550-nm resonance wavelength of the gold virus (i.e., 7 nm) are presented in blue and dark blue, respectively. (**d**) The detection of the vibrational (or Raman) spectrum of a conventional Raman dye molecule, 1,2-bis(4-pyridyl)ethylene, *via* CPMVs coated with 2 nm of gold. The gold virus enabled the sensitive detection of fingerprint information at Raman shifts of 1200, 1615 and 1635 cm^{-1} at a picomolar concentration. The control samples consisted of similar-sized nanospheres with 2-nm-thick and 4-nm-thick gold layers, corresponding to the same gold thickness as that of the gold virus and the same 785-nm resonance as that of the gold virus; the results for these two samples are presented in blue and dark blue, respectively. (**e**) Comparison of Raman scattering intensities at the 1615 cm^{-1} peak. The gold virus exhibited a greater sensitivity by six orders of magnitude. CPMV, cow pea mosaic virus; cyt c, cytochrome c.

Raman detection, BPE was selected as the target molecule to avoid overlap between the excitation wavelength and the molecular electron transition.[50] CPMVs coated with 2 nm of gold, 33-nm nanospheres with the same gold thickness and 33-nm nanospheres coated with 4-nm-thick gold layers to achieve resonance at 785 nm were tested in 785-nm laser excitation Raman measurements because these particles exhibited resonances near the excitation wavelength (Supplementary Fig. S3). The gold-coated CPMV particles achieved clear detection at subpicomolar concentrations of BPE, whereas the gold-coated nanospheres could detect concentrations only down to the micromolar level. A direct comparison of the detection limits indicates that the three-dimensional folded viral capsid yielded a 10^6-fold higher sensitivity compared to the smooth nanospheres. Moreover, the Raman signals were temporally stable, with less than 10% deviation, even at the lowest concentrations. Blinking, which is commonly observed at single-molecule-level concentrations,[3] was not observed in gold-virus-based detection, which may suggest the occurrence of molecular preconcentration around the nanoscale morphology.[51]

CONCLUSION

In conclusion, we demonstrated biologically inspired optical antennas using plant viruses for molecular absorption and vibration imaging. We utilized three-dimensional viral capsids as templates for the optical antennas and experimentally demonstrated the high sensitivity of these antennas for nanospectroscopic molecular imaging. In addition to the benefits of the subnanoscale topology of virus capsids, the diversity of virus morphologies in nature and their shape homogeneity and high-throughput reproducibility enhance the potential for the use of viral particles in optical sensing applications. Furthermore, by means of asymmetric gold conjugation that leaves parts of the native capsid exposed, gold viruses can exhibit both inherent viral functions (i.e., interactions with host cells) and biochemically modified functions, including subcellular targeting, imaging-agent loading, and drug-carrying capability. Thus, such gold virus nanoparticles can metaphorically serve as 'nanosatellites' exploring 'cellular galaxies'.

ACKNOWLEDGEMENTS

This work was supported by the Air Force Office of Scientific Research Grants AFOSR FA2386-13-1-4120.

1 Barnes WL, Dereux A, Ebbesen TW. Surface plasmon subwavelength optics. *Nature* 2003; **424**: 824–830.
2 Kawata S, Inouye Y, Verma P. Plasmonics for near-field nano-imaging and superlensing. *Nat Photonics* 2009; **3**: 388–394.
3 Nie SM, Emery SR. Probing single molecules and single nanoparticles by surface-enhanced Raman scattering. *Science* 1997; **275**: 1102–1106.
4 Liu GL, Long YT, Choi Y, Kang T, Lee LP. Quantized plasmon quenching dips nanospectroscopy *via* plasmon resonance energy transfer. *Nat Methods* 2007; **4**: 1015–1017.

doi:10.1038/lsa.2015.40

5 Kim S, Jin JH, Kim YJ, Park IY, Kim Y *et al*. High-harmonic generation by resonant plasmon field enhancement. *Nature* 2008; **453**: 757–760.
6 Pu Y, Grange R, Hsieh CL, Psaltis D. Nonlinear optical properties of core–shell nanocavities for enhanced second-harmonic generation. *Phys Rev Lett* 2010; **104**: 207402.
7 Morfa AJ, Rowlen KL, Reilly TH, Romero MJ, van de Lagemaat J. Plasmon-enhanced solar energy conversion in organic bulk heterojunction photovoltaics (vol 92, 013504, 2008). *Appl Phys Lett* 2008; **92**: 013504.
8 Ozbay E. Plasmonics: merging photonics and electronics at nanoscale dimensions. *Science* 2006; **311**, 189–193.
9 Shalaev VM. Optical negative-index metamaterials. *Nat Photonics* 2007; **1**: 41–48.
10 Zijlstra P, Paulo PMR, Orrit M. Optical detection of single non-absorbing molecules using the surface plasmon resonance of a gold nanorod. *Nat Nanotechnol* 2012; **7**: 379–382.
11 Tkachenko AG, Xie H, Coleman D, Glomm W, Ryan J *et al*. Multifunctional gold nanoparticle–peptide complexes for nuclear targeting. *J Am Chem Soc* 2003; **125**: 4700–4701.
12 Agasti SS, Chompoosor A, You CC, Ghosh P, Kim CK *et al*. Photoregulated release of caged anticancer drugs from gold nanoparticles. *J Am Chem Soc* 2009; **131**: 5728.
13 Lewis JD, Destito G, Zijlstra A, Gonzalez MJ, Quigley JP *et al*. Viral nanoparticles as tools for intravital vascular imaging. *Nat Med* 2006; **12**: 354–360.
14 Singh P, Prasuhn D, Yeh RM, Destito G, Rae CS *et al*. Bio-distribution, toxicity and pathology of cowpea mosaic virus nanoparticles *in vivo*. *J Control Release* 2007; **120**: 41–50.
15 Rae CS, Khor IW, Wang Q, Destito G, Gonzalez MJ *et al*. Systemic trafficking of plant virus nanoparticles in mice *via* the oral route. *Virology* 2005; **343**: 224–235.
16 Ren Y, Wong SM, Lim LY. Folic acid-conjugated protein cages of a plant virus: a novel delivery platform for doxorubicin. *Bioconjugate Chem* 2007; **18**: 836–843.
17 Klimstra WB, Williams JC, Ryman KD, Heidner HW. Targeting Sindbis virus-based vectors to F*c* receptor-positive cell types. *Virology* 2005; **338**: 9–21.
18 Douglas T, Young M. Host–guest encapsulation of materials by assembled virus protein cages. *Nature* 1998; **393**: 152–155.
19 Comellas-Aragones M, Engelkamp H, Claessen VI, Sommerdijk NAJM, Rowan AE *et al*. A virus-based single-enzyme nanoreactor. *Nat Nanotechnol* 2007; **2**: 635–639.
20 Canizares MC, Nicholson L, Lomonossoff GP. Use of viral vectors for vaccine production in plants. *Immunol Cell Biol* 2005; **83**: 263–270.
21 Scholthof HB, Scholthof KBG, Jackson AO. Plant virus gene vectors for transient expression of foreign proteins in plants. *Annu Rev Phytopathol* 1996; **34**: 299–323.
22 Miller RA, Presley AD, Francis MB. Self-assembling light-harvesting systems from synthetically modified tobacco mosaic virus coat proteins. *J Am Chem Soc* 2007; **129**: 3104–3109.
23 Endo M, Fujitsuka M, Majima T. Porphyrin light-harvesting arrays constructed in the recombinant tobacco mosaic virus scaffold. *Chem Eur J* 2007; **13**: 8660–8666.
24 Nam KT, Kim DW, Yoo PJ, Chiang CY, Meethong N *et al*. Virus-enabled synthesis and assembly of nanowires for lithium ion battery electrodes. *Science* 2006; **312**: 885–888.
25 Tseng RJ, Tsai C, Ma L, Ouyang J, Ozkan CS *et al*. Digital memory device based on tobacco mosaic virus conjugated with nanoparticles. *Nat Nanotechnol* 2006; **1**: 72–77.
26 Zandi R, Reguera D, Bruinsma RF, Gelbart WM, Rudnick J. Origin of icosahedral symmetry in viruses. *Proc Natl Acad Sci USA* 2004; **101**: 15556–15560.
27 Wang Q, Kaltgrad E, Lin TW, Johnson JE, Finn MG. Natural supramolecular building blocks: wild-type cowpea mosaic virus. *Chem Biol* 2002; **9**: 805–811.
28 Young M, Willits D, Uchida M, Douglas T. Plant viruses as biotemplates for materials and their use in nanotechnology. *Annu Rev Phytopathol* 2008; **46**: 361–384.
29 Baker TS, Olson NH, Fuller SD. Adding the third dimension to virus life cycles: Three-dimensional reconstruction of icosahedral viruses from cryo-electron micrographs. *Microbiol Mol Biol Rev* 1999; **63**: 862.
30 Liang HY, Li, ZP, Wang WZ, Wu YS, Xu HX. Highly surface-roughened ''flower-like'' silver nanoparticles for extremely sensitive substrates of surface-enhanced raman scattering. *Adv Mater* 2009; **21**: 4614–4618.
31 Wu LY, Ross, BM, Hong S, Lee LP. Bioinspired nanocorals with decoupled cellular targeting and sensing functionality. *Small* 2010; **6**: 503–507.
32 Muhlschlegel P, Eisler HJ, Martin OJF, Hecht B, Pohl DW. Resonant optical antennas. *Science* 2005; **308**: 1607–1609.
33 van Kammen A. Purification and properties of the components of cowpea mosaic virus. *Virology* 1967; **31**: 633–642.
34 Andersson S. The structure of virus capsids. *Z Anorg Allg Chem* 2008; **634**: 2161–2170.
35 Etchegoin PG, Le Ru EC, Meyer M. An analytic model for the optical properties of gold. *J Chem Phys* 2006; **125**: 164705.
36 Jackson JD. *Classical Electrodynamics*. New York: Wiley; 1999.
37 Huxley HE, Zubay G. Preferential staining of nucleic acid-containing structures for electron microscopy. *J Biophys Biochem Cytol* 1961; **11**: 273.
38 Hulteen JC, Young MA, van Duyne RP. Surface-enhanced hyper-Raman scattering (SEHRS) on Ag film over nanosphere (FON) electrodes: surface symmetry of centrosymmetric adsorbates. *Langmuir* 2006; **22**: 10354–10364.
39 Adrian M, Dubochet J, Lepault J, Mcdowall AW. Cryo-electron microscopy of viruses. *Nature* 1984; **308**: 32–36.
40 Haes AJ, Zou S, Zhao J, Schatz GC, van Duyne RP. Localized surface plasmon resonance spectroscopy near molecular resonances. *J Am Chem Soc* 2006; **128**: 10905–10914.
41 Plummer EM, Manchester M. Endocytic uptake pathways utilized by CPMV nanoparticles. *Mol Pharm* 2013; **10**: 26–32.
42 Caspar DL, Klug A. Physical principles in the construction of regular viruses. *Cold Spring Harb Symp Quant Biol* 1962; **27**: 1–24.
43 Twarock R. Mathematical virology: a novel approach to the structure and assembly of viruses. *Philos Trans R Soc A* 2006; **364**: 3357–3373.
44 Xu HX, Aizpurua J, Kall M, Apell P. Electromagnetic contributions to single-molecule sensitivity in surface-enhanced Raman scattering. *Phys Rev E* 2000; **62**: 4318–4324.
45 Link S, Burda C, Mohamed MB, Nikoobakht B, El-Sayed MA. Laser photothermal melting and fragmentation of gold nanorods: energy and laser pulse-width dependence. *J Phys Chem A* 1999; **103**: 1165–1170.
46 Bruening G, Buzayan JM, Ferreiro C, Lim W. Evidence for participation of RNA 1-encoded elicitor in Cowpea mosaic virus-mediated concurrent protection. *Virology* 2000; **266**: 299–309.
47 Choi YH, Kang T, Lee LP. Plasmon resonance energy transfer (PRET)-based molecular imaging of cytochrome c in living cells. *Nano Lett* 2009; **9**: 85–90.
48 Choi Y, Park Y, Kang T, Lee LP. Selective and sensitive detection of metal ions by plasmonic resonance energy transfer-based nanospectroscopy. *Nat Nanotechnol* 2009; **4**: 742–746.
49 Schatz GC, Young MA, van Duyne RP. Electromagnetic mechanism of SERS. *Top Appl Phys* 2006; **103**: 19–45.
50 Dick LA, Haes AJ, van Duyne RP. Distance and orientation dependence of heterogeneous electron transfer: a surface-enhanced resonance Raman scattering study of cytochrome c bound to carboxylic acid terminated alkanethiols adsorbed on silver electrodes. *J Phys Chem B* 2000; **104**: 11752–11762.
51 Kang T, Hong S, Choi Y, Lee LP. The effect of thermal gradients in SERS spectroscopy. *Small* 2010; **6**: 2649–2652.

Supplementary information for this article can be found on the *Light: Science & Applications*' website (http://www.nature.com/lsa/).